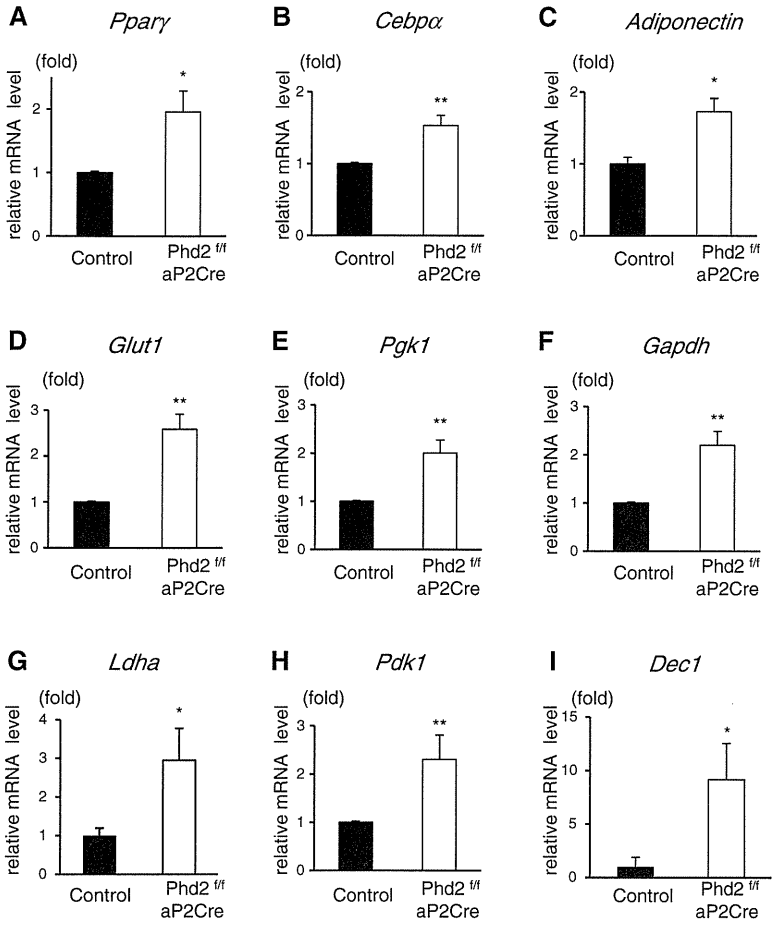

Figure 4. Expression of adipocyte differentiation markers and glycolytic enzymes was increased in the adipocyte-rich fraction from *Phd2$^{f/f}$/aP2-Cre* mice. Total RNA was extracted from the adipocyte-rich fraction of high-fat diet–fed control and *Phd2$^{f/f}$/aP2-Cre* mice. The results of real-time quantitative polymerase chain reaction analyses for (**A**) peroxisome proliferator activated receptor-γ (*Pparγ*), (**B**) CCAAT/enhancer binding protein α (*Cebpα*), (**C**) adiponectin, (**D**) glucose transporter 1 (*Glut1*), (**E**) phosphoglycerate kinase 1 (*Pgk1*), (**F**) glyceraldehyde-3-phosphate dehydrogenase (*Gapdh*), (**G**) lactate dehydrogenasea (*Ldha*), (**H**) pyruvate dehydrogenase kinase 1 (*Pdk1*), and (**I**) DEC-1/Stra13 are shown in the bar graphs. n=6. *P<0.05, **P<0.01 vs control.

Adipocyte Differentiation Markers and Glycolytic Enzymes Were Increased in Isolated Adipocytes of WAT in HFD-Fed *Phd2$^{f/f}$/aP2-Cre* Mice

We determined the expression of adipogenic markers in an adipocyte-rich fraction isolated from WAT of *Phd2$^{f/f}$/aP2-Cre* mice and controls to exclude the effect of stromal vascular cells. The expression of peroxisome proliferator-activated receptor-γ (*Pparγ*), CCAAT/enhancer binding protein α (*Cebp* α), and adiponectin was increased in the adipocyte-rich fraction of HFD-fed *Phd2$^{f/f}$/aP2-Cre* mice (Figure 4A–4C). However, the serum adiponectin concentration was not significantly different between control and *Phd2$^{f/f}$/aP2-Cre* mice (Figure III in the online-only Data Supplement).

Expression of Glucose Transporter and Glycolytic Enzymes Was Upregulated in Isolated Adipocytes From WAT of HFD-Fed *Phd2$^{f/f}$/aP2-Cre* Mice

Because HIF is known to activate glycolytic pathway,[17] we analyzed the expression of genes involved in glycolysis. The expression of glucose transporter 1 (*Glut1*) and several glycolytic enzymes such as phosphoglycerate kinase (*Pgk1*), glyceraldehyde-3-phosphate dehydrogenase (*Gapdh*), and lactate dehydrogenase-a (*Ldha*) was significantly upregulated in the adipocyte-rich fraction isolated from WAT of *Phd2$^{f/f}$/aP2-Cre* mice (Figure 4D–4G). In addition, the expression of pyruvate dehydrogenase kinase 1 (*Pdk1*), a rate-limiting enzyme of oxidative phosphorylation, was also significantly upregulated (Figure 4H). *Dec1*, which inhibits adipogenesis,[13] was also upregulated in *Phd2$^{f/f}$/aP2-Cre* mice (Figure 4I).

Unexpectedly, however, the serum lactate level was rather decreased in HFD-fed *Phd2$^{f/f}$/aP2-Cre* mice despite the upregulated expression of glycolytic enzymes (Table). We examined LDHa protein expression and found that LDHa protein was actually increased in WAT of *Phd2$^{f/f}$/aP2-Cre* mice (Figure IVA in the online-only Data Supplement).

Phd2$^{f/f}$/aP2-Cre Mice Showed Increased Oxygen Consumption With Uncoupling Protein-1 Upregulation

Oxygen consumption (Vo_2) was significantly increased in HFD-fed *Phd2$^{f/f}$/aP2-Cre* mice in both the light and dark periods (Figure 5A). Carbon dioxide production (Vco_2) was slightly increased in *Phd2$^{f/f}$/aP2-Cre* mice, but the difference was not statistically significant (Figure 5B). The respiratory exchange ratio was significantly lower in *Phd2$^{f/f}$/aP2-Cre* mice during the dark period when mice were active, but there was no difference during the light period (Figure 5C). The expression of *Ucp1*, one of the critical genes controlling the energy expenditure, was significantly upregulated in HFD-fed PHD2-deficient BAT compared with controls (Figure 5D). These data suggest that *PHD2* deletion in adipocytes increased energy expenditure using lipid at least partly mediated by upregulation of *Ucp1* in BAT.

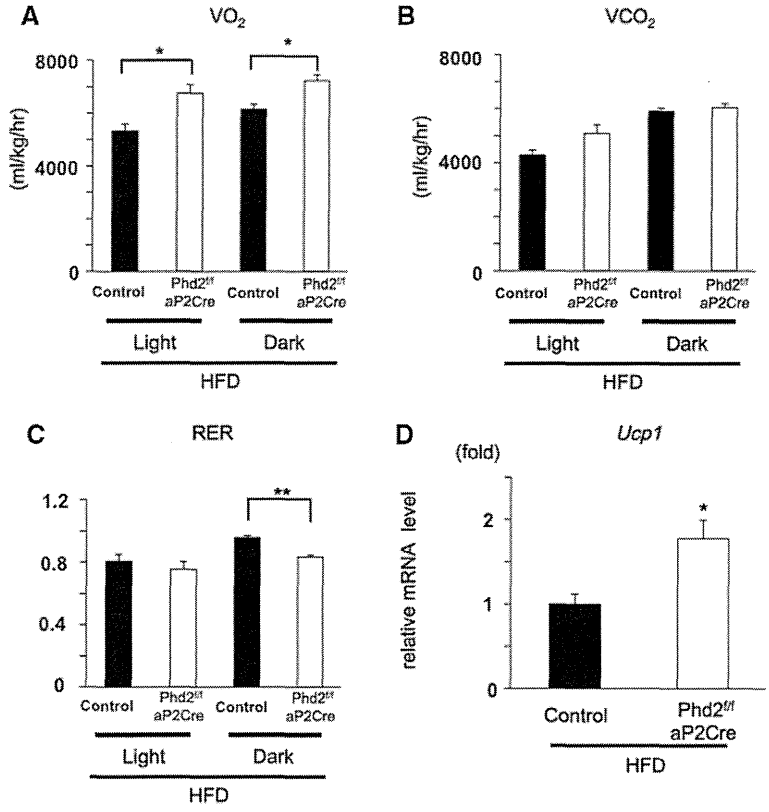

Figure 5. Oxygen consumption was increased in *Phd2$^{f/f}$/aP2-Cre* mice. **A** through **C,** High-fat diet (HFD)–fed control and *Phd2$^{f/f}$/aP2-Cre* mice were housed in a computer-controlled open-circuit indirect calorimeter to determine (**A**) oxygen consumption, (**B**) carbon dioxide production, and (**C**) respiratory exchange ratio (RER) during the light (8 am–8 pm) and dark (8 pm–8 am) periods. n=3. *P<0.05, **P<0.01. **D,** The result of real-time quantitative polymerase chain reaction analysis for uncoupling protein-1 (*Ucp*-1) in brown adipose tissue from HFD-fed control and *Phd2$^{f/f}$/aP2-Cre* mice is shown in the bar graph. n=6, *P<0.05 vs control.

Glut4 in Skeletal Muscle in *Phd2$^{f/f}$/aP2-Cre* Mice Was Upregulated

The expression of *Glut4* in skeletal muscle (quadriceps femoris muscle) of *Phd2$^{f/f}$/aP2-Cre* mice was significantly upregulated compared with controls (Figure 6A). Because Glut4 is downstream of insulin signaling, we examined the insulin signaling pathway in skeletal muscle. Expression of Glut4 protein and phosphorylation of Akt were increased in *Phd2$^{f/f}$/aP2-Cre* mice, which may support the idea that insulin sensitivity is improved in *Phd2$^{f/f}$/aP2-Cre* mice (Figure IVB in the online-only Data Supplement). The expression of genes involved in fatty acid oxidation such as acyl-CoA oxidase, carnitine palmitoyltransferase-1, and medium-chain acyl-CoA dehydrogenase in skeletal muscle was comparable between controls and *Phd2$^{f/f}$/aP2-Cre* mice, suggesting that fatty acid oxidation was not increased in skeletal muscle of *Phd2$^{f/f}$/aP2-Cre* mice (Figure 6B–6D). The expression of genes involved in hepatic gluconeogenic enzymes such as phosphoenolpyruvate carboxykinase and glucose-6-phosphatase was not different between the 2 mouse groups, suggesting that gluconeogenesis in the liver is not affected by *PHD2* deletion in the adipocytes (Figure 6E and 6F).

Glycolysis Was Promoted and Lipid Accumulation Was Suppressed in PHD2-Deficient 3T3-L1 Cells

To confirm that PHD2 deficiency increases glycolysis and attenuates lipid accumulation in adipocytes, we specifically knocked down *Phd2* mRNA by *Phd2*-specific shRNA in 3T3-L1 cells. The expression of both *Phd2* mRNA and PHD2 protein was significantly decreased in PHD2-deficient 3T3-L1 preadipocytes (Figure 7A and 7B). Hypoxia responsive element–dependent luciferase activity was significantly increased (Figure 7C).

In agreement with the results of in vivo experiments, the expression of *Glut1*, *Pgk1*, *Gapdh*, *Ldha*, and *Pdk1* was significantly upregulated in PHD2-deficient 3T3-L1 preadipocytes (Figure 7D). After the induction of adipocyte differentiation, the expression of Glut1 was reduced in PHD2-deficient 3T3-L1 adipocytes, whereas the expression of other genes was still significantly upregulated (Figure 7E). Both glucose consumption and lactate production in the supernatant were significantly increased in PHD2-deficient 3T3-L1 preadipocytes compared with control 3T3-L1 preadipocytes (Figure 7F and 7G), indicating acceleration of glycolysis. We also assessed de novo lipogenesis because PDK1 suppresses acetyl-CoA production, which is essential for fatty acid synthesis.[25] Oil Red O staining revealed that PHD2-deficient 3T3-L1 cells accumulated less lipid than control 3T3L-1 cells (Figure 7H and 7I).

Discussion

In this study, we demonstrated that *PHD2* deletion in adipocyte alleviates diet-induced obesity and glucose intolerance in mice. *PHD2* deletion reduced fat mass and macrophage infiltration into WAT and increased the expression of UCP-1 in BAT and oxygen consumption, all of which are supposed to be responsible for body weight reduction and better glucose tolerance in HFD-fed *Phd2$^{f/f}$/aP2-Cre* mice. The improvement in the glucose tolerance test was remarkable compared with the improvement in the insulin tolerance test under HFD, indicating that an improvement of insulin sensitivity may not be the

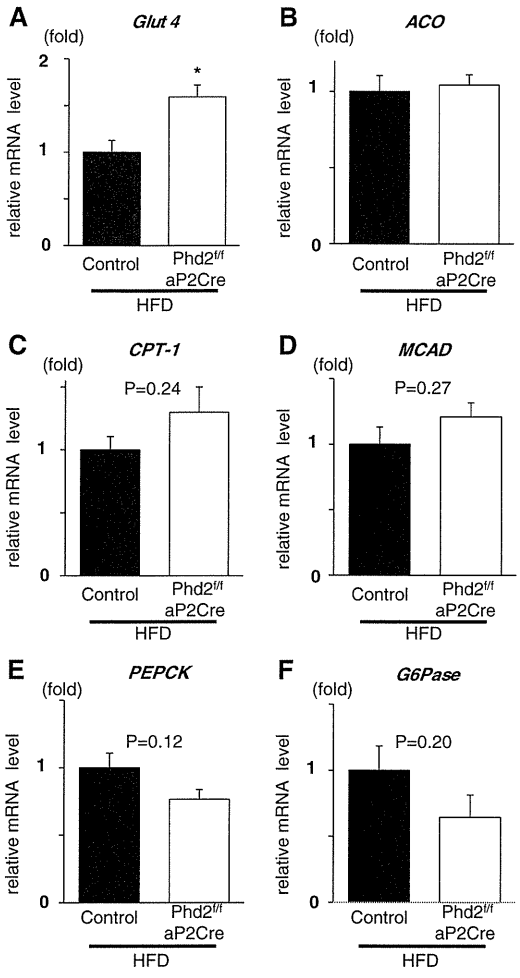

Figure 6. Glucose transporter 4 (Glut4) in skeletal muscle in *Phd2$^{f/f}$/aP2-Cre* mice was upregulated. **A** through **D**, Total RNA was extracted from skeletal muscle (quadriceps femoris muscle) of high-fat diet (HFD)–fed control and *Phd2$^{f/f}$/aP2-Cre* mice. The results of real-time quantitative polymerase chain reaction (qPCR) analyses for (**A**) *Glut4,* (**B**) acyl-CoA oxidase (*ACO*), (**C**) carnitine palmitoyltransferase-1 (*CPT-1*), and (**D**) medium-chain acyl-CoA dehydrogenase (*MCAD*) are shown in the bar graphs. n=6. *$P<0.05$ vs control. **E** and **F**, Total RNA was extracted from liver of HFD-fed control and *Phd2$^{f/f}$/aP2-Cre* mice. The results of real-time qPCR analyses for (**E**) phosphoenolpyruvate carboxykinase (*PEPCK*) and (**F**) glucose-6-phosphatase (*G6Pase*) are shown in the bar graphs. n=6.

primary effect of PHD2 deficiency. However, improvement in the homeostasis model assessment–insulin resistance suggests that insulin sensitivity in *Phd2$^{f/f}$/aP2-Cre* mice may be improved to some extent. These data also suggest that PHD2 inhibition may improve glucose metabolism in the presence of insulin resistance.

Phd2$^{f/f}$/aP2-Cre mice showed several beneficial morphological features of adipose tissue. First, the size of adipocytes in PHD2-deficient WAT was reduced. It is generally accepted that better glucose tolerance is associated with smaller adipocyte size and conversely that hypertrophied adipocytes are strongly linked to insulin resistance.[2] Second, macrophage infiltration into WAT was significantly suppressed in *Phd2$^{f/f}$/aP2-Cre* mice. Although the causal relationship might be difficult to determine, alteration of morphological features by *PHD2* deletion should cause better glucose tolerance and insulin sensitivity.

Although hypoxia has been known to reduce body weight[9] and fat mass,[26–28] it is intriguing that even PHD2 deletion in adipocytes showed a similar effect. In PHD2-deficient adipocytes, the glycolytic pathway becomes dominant because of the HIF-induced expression of glucose transporter and glycolytic enzymes, which is often called aerobic glycolysis.[29] Glycolysis is an inefficient way to produce energy compared with oxidative phosphorylation. Hence, the cells depending on glycolysis consume more glucose wastefully compared with those depending on oxidative phosphorylation when both cell types are required to generate an equal amount of ATP.[30] Therefore, PHD2-deficient adipocytes may consume more glucose than normal adipocytes. Although an in vitro study showed that PHD2 knockdown increases lactate production in the supernatant, the serum lactate level was rather decreased in *Phd2$^{f/f}$/aP2-Cre* mice. The reason for this discrepancy is not clear but may be due to a reduction in adiposity in *Phd2$^{f/f}$/aP2-Cre* mice. Because HFD loading increased serum lactate levels even in control mice (Table), the decrease in lactate levels in *Phd2$^{f/f}$/aP2-Cre* mice may reflect the reduced total adipose tissue mass.

PHD2 deletion attenuated fatty acid synthesis possibly through *Pdk1* upregulation. PDK1 suppresses the activity of pyruvate dehydrogenase, which catalyzes the conversion of pyruvate to acetyl CoA, an essential substrate for de novo fatty acid synthesis.[25] As a result, lipogenesis is expected to be reduced. In addition, *PHD2* deletion in adipocytes may enhance lipid consumption. *Phd2$^{f/f}$/aP2-Cre* mice consumed more oxygen with a lower respiratory exchange ratio and showed reduced lipid content in BAT, which may be explained, at least in part, by the upregulation of *Ucp1* expression. However, the detailed mechanism for UCP-1 upregulation is not clear at this point because UCP-1 is not a target gene of HIF. Overall, *PHD2* deletion–associated reprogramming of glucose and lipid metabolism might contribute to obesity resistance.

It is reported that hypoxia inhibits adipogenesis through upregulation of DEC1.[13] DEC1 is a transcription factor induced by HIF-1α that suppresses peroxisome proliferator–activated receptor-γ expression, resulting in the inhibition of adipogenesis. DEC1 expression in adipose tissue from *Phd2$^{f/f}$/aP2-Cre* mice was increased. However, peroxisome proliferator–activated receptor-γ expression is rather increased in WAT from *Phd2$^{f/f}$/aP2-Cre* mice (Figure 4A). Therefore, it is unlikely that DEC1 is involved in the reduced adiposity in *Phd2$^{f/f}$/aP2-Cre* mice.

Unexpectedly, we have found that Akt phosphorylation and Glut4 expression in the skeletal muscle of *Phd2$^{f/f}$/aP2-Cre* mice were increased. These data may suggest that insulin sensitivity is improved in HFD-fed *Phd2$^{f/f}$/aP2-Cre* mice compared with HFD-fed control mice. It is reported that Glut4 expression in skeletal muscle is suppressed in a rat model of insulin resistance,[31] suggesting that Glut4 upregulation in *Phd2$^{f/f}$/aP2-Cre* mice may be due to an improvement in insulin sensitivity. However, it is not clear how PHD2 deficiency in adipocytes affects the skeletal muscle insulin signaling pathway; further study is needed.

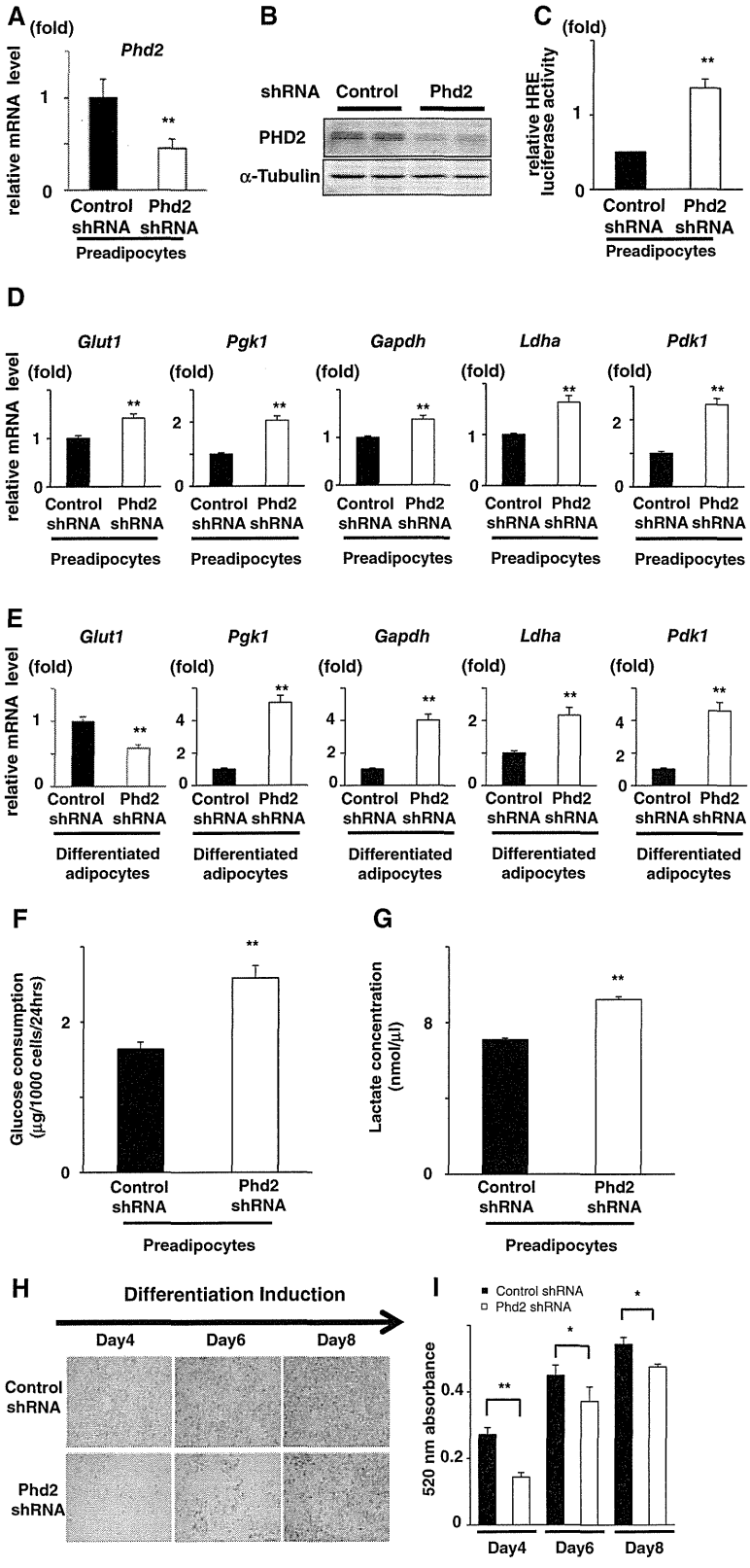

Figure 7. Knockdown of prolyl hydroxylase domain protein 2 (PHD2) in 3T3-L1 cells induced enhancement of glycolysis and attenuation of lipid accumulation. **A,** Total RNA was extracted from control shRNA and Phd2 shRNA expressing 3T3-L1 preadipocytes. The result of real-time quantitative polymerase chain reaction (qPCR) analyses for *Phd2* is shown in the bar graph. n=4. ** $P<0.01$ vs control shRNA. **B,** Western blot analysis for PHD2 and α-tubulin using total cell lysates of control shRNA and Phd2 shRNA expressing 3T3-L1 preadipocytes is shown. The same results were obtained in other independent experiments. n=3. **C,** The luciferase activity after 24 hours of transfection of a hypoxia responsive element (HRE)–luciferase vector into control shRNA and Phd2 shRNA expressing 3T3-L1 preadipocytes is shown in the bar graph. n=3. **$P<0.01$ vs control shRNA. **D** and **E,** Total RNA was extracted from control and Phd2 shRNA expressing 3T3-L1 preadipocytes (**D**) and differentiated 3T3-L1 adipocytes (**E**). The results of real-time qPCR analyses for glucose transporter 1 (*Glut1*), phosphoglycerate kinase 1 (*Pgk1*), glyceraldehyde-3-phosphate dehydrogenase (*Gapdh*), lactate dehydrogenase a (*Ldha*), and pyruvate dehydrogenase kinase 1 (*Pdk1*) are shown in the bar graph. n=4. **$P<0.01$ vs control shRNA. **F** and **G,** Glucose consumption (**F**) and lactate concentration (**G**) in the culture media of control shRNA and Phd2 shRNA expressing 3T3-L1 preadipocytes after 24 hours of incubation are shown in the bar graphs. n=4. **$P<0.01$ vs control shRNA. **H,** Control shRNA and Phd2 shRNA expressing 3T3-L1 cells were differentiated, and lipid accumulation in the cytosol was determined by Oil Red O staining. Representative pictures of 4 independent experiments at 4, 6, and 8 days of differentiation are shown. **I,** Quantification of Oil Red O contents of control shRNA (black bar) and Phd2 shRNA (white bar) expressing 3T3-L1 cells is shown in the bar graph. n=3. *$P<0.05$, **$P<0.01$ vs control shRNA.

It is known that adipose tissue in obese patients is subjected to hypoxia and HIF is accumulated,[32–34] which is explained by the facts that hypertrophied adipocytes become physically distant from capillaries and that inflammatory cells infiltrating into adipose tissue consume a substantial amount of oxygen. However, it has not been determined whether hypoxia in obese adipose tissue plays a causative role in obesity-associated metabolic abnormalities.[33,35] Recently, adipocyte-specific HIF-1α transgenic mice have been reported.[36] The transgenic mice gained more body weight than controls on both normal diet

and an HFD, showing glucose intolerance and insulin resistance. The adipose tissue in HIF-1α transgenic mice developed more fibrosis in association with local inflammation. These phenotypes are opposite of our observation. We observed that PHD2 deficiency with increased HIF-1α and HIF-2α neither led to adipocyte hypertrophy or local inflammation nor worsened HFD-induced obesity and glucose intolerance. The reason for this discrepancy is not immediately clear at this stage, but one of the differences between the previous study and our study is upregulation of HIF-2α in adipocytes in *Phd2$^{f/f}$/aP2-Cre* mice. Interestingly, HIF-1α and HIF-2α have opposite effects on adipogenesis: HIF-1α inhibits adipogenesis[13] and HIF-2α promotes it.[37] Therefore, the net effects by PHD2 inhibition on adipose tissue formation may be more complicated than the consequence of a single HIF-1α overexpression. Another possibility is that there may be unidentified substrates of PHD2 for hydroxylation that may be related to glucose and lipid metabolism and inflammation. In contrast, our observation is supported by several lines of evidence from genetically modified mice.[30,38,39] Overexpression of a dominant-negative form of HIF-1α in adipocytes accelerated HFD-induced glucose intolerance and insulin resistance and induced more severe obesity.[38] Another study showed that factor inhibiting HIF-1α–deficient mice that have elevated HIF activity are also resistant to HFD-induced body weight gain and glucose intolerance.[39] This evidence consistently suggests that HIF signaling is positively linked to resistance to obesity and associated metabolic abnormalities. It is of note that our study revealed that inhibition of PHD2 in adipocytes sufficiently attenuated HFD-induced glucose intolerance and obesity without an increase in serum lactate level, which is observed in SIRT6-deficient mice.[30] Therefore, inhibition of PHD in adipocytes might be meritorious in terms of clinical application.

The limitation of the present study is that we have not excluded the possible involvement of PHD2-deficient macrophages because the *aP2* gene is known to be expressed in not only adipocytes but also macrophages.[40] However, the reduction in PHD2 expression in bone marrow–derived macrophages or stromal vascular fraction that is rich in macrophages in *Phd2$^{f/f}$/aP2-Cre* mice was modest and not so remarkable compared with that in adipocytes. Therefore, the effect of PHD2-deletion in macrophages may play a relatively minor role in the reduction of fat mass and the improvement in glucose metabolism in *Phd2$^{f/f}$/aP2-Cre* mice.

Conclusions

We showed in this study that PHD2 in adipocytes plays a multifaceted role in the regulation of metabolism and inflammation in diet-induced obesity. Adipocyte-specific *Phd2* deletion ameliorates diet-induced obesity and several obesity-associated metabolic abnormalities. Thus, PHD2 in adipocytes may be a novel target for the treatment of patients with metabolic syndrome.

Acknowledgments

We acknowledge the technical expertise of the Support Center for Education and Research, Kyushu University.

Sources of Funding

This work was supported in part by a Grant-in-Aid for Scientific Research from the Ministry of Education, Culture, Sports, Science, and Technology of Japan (19590867 to Dr Ichiki) and research grant 2010 from AstraZeneca, SENSHIN Medical Research Foundation, Japanese Foundation for Applied Enzymology, and Takeda Medical Research Foundation to Dr Ichiki.

Disclosures

None.

References

1. Van Gaal LF, Mertens IL, De Block CE. Mechanisms linking obesity with cardiovascular disease. *Nature*. 2006;444:875–880.
2. Hotamisligil GS. Inflammation and metabolic disorders. *Nature*. 2006;444:860–867.
3. Martínez JA. Mitochondrial oxidative stress and inflammation: an slalom to obesity and insulin resistance. *J Physiol Biochem*. 2006;62:303–306.
4. Ozcan U, Cao Q, Yilmaz E, Lee AH, Iwakoshi NN, Ozdelen E, Tuncman G, Görgün C, Glimcher LH, Hotamisligil GS. Endoplasmic reticulum stress links obesity, insulin action, and type 2 diabetes. *Science*. 2004;306:457–461.
5. Nishimura S, Manabe I, Nagasaki M, Eto K, Yamashita H, Ohsugi M, Otsu M, Hara K, Ueki K, Sugiura S, Yoshimura K, Kadowaki T, Nagai R. CD8+ effector T cells contribute to macrophage recruitment and adipose tissue inflammation in obesity. *Nat Med*. 2009;15:914–920.
6. Cooke D, Bloom S. The obesity pipeline: current strategies in the development of anti-obesity drugs. *Nat Rev Drug Discov*. 2006;5:919–931.
7. Després JP, Golay A, Sjöström L; Rimonabant in Obesity-Lipids Study Group. Effects of rimonabant on metabolic risk factors in overweight patients with dyslipidemia. *N Engl J Med*. 2005;353:2121–2134.
8. Christensen R, Kristensen PK, Bartels EM, Bliddal H, Astrup A. Efficacy and safety of the weight-loss drug rimonabant: a meta-analysis of randomised trials. *Lancet*. 2007;370:1706–1713.
9. Shukla V, Singh SN, Vats P, Singh VK, Singh SB, Banerjee PK. Ghrelin and leptin levels of sojourners and acclimatized lowlanders at high altitude. *Nutr Neurosci*. 2005;8:161–165.
10. Allahdadi KJ, Walker BR, Kanagy NL. Augmented endothelin vasoconstriction in intermittent hypoxia-induced hypertension. *Hypertension*. 2005;45:705–709.
11. Simler N, Grosfeld A, Peinnequin A, Guerre-Millo M, Bigard AX. Leptin receptor-deficient obese Zucker rats reduce their food intake in response to hypobaric hypoxia. *Am J Physiol Endocrinol Metab*. 2006;290:E591–E597.
12. Quintero P, Milagro FI, Campión J, Martínez JA. Impact of oxygen availability on body weight management. *Med Hypotheses*. 2010;74:901–907.
13. Yun Z, Maecker HL, Johnson RS, Giaccia AJ. Inhibition of PPAR gamma 2 gene expression by the HIF-1-regulated gene DEC1/Stra13: a mechanism for regulation of adipogenesis by hypoxia. *Dev Cell*. 2002;2:331–341.
14. Kaelin WG Jr, Ratcliffe PJ. Oxygen sensing by metazoans: the central role of the HIF hydroxylase pathway. *Mol Cell*. 2008;30:393–402.
15. Semenza GL, Roth PH, Fang HM, Wang GL. Transcriptional regulation of genes encoding glycolytic enzymes by hypoxia-inducible factor 1. *J Biol Chem*. 1994;269:23757–23763.
16. Semenza GL, Jiang BH, Leung SW, Passantino R, Concordet JP, Maire P, Giallongo A. Hypoxia response elements in the aldolase A, enolase 1, and lactate dehydrogenase A gene promoters contain essential binding sites for hypoxia-inducible factor 1. *J Biol Chem*. 1996;271:32529–32537.
17. Kim JW, Tchernyshyov I, Semenza GL, Dang CV. HIF-1-mediated expression of pyruvate dehydrogenase kinase: a metabolic switch required for cellular adaptation to hypoxia. *Cell Metab*. 2006;3:177–185.
18. Papandreou I, Cairns RA, Fontana L, Lim AL, Denko NC. HIF-1 mediates adaptation to hypoxia by actively downregulating mitochondrial oxygen consumption. *Cell Metab*. 2006;3:187–197.
19. Fraisl P, Aragonés J, Carmeliet P. Inhibition of oxygen sensors as a therapeutic strategy for ischaemic and inflammatory disease. *Nat Rev Drug Discov*. 2009;8:139–152.
20. Berra E, Benizri E, Ginouvès A, Volmat V, Roux D, Pouysségur J. HIF prolyl-hydroxylase 2 is the key oxygen sensor setting low steady-state levels of HIF-1alpha in normoxia. *EMBO J*. 2003;22:4082–4090.
21. Takeda K, Ho VC, Takeda H, Duan LJ, Nagy A, Fong GH. Placental but not heart defects are associated with elevated hypoxia-inducible factor

alpha levels in mice lacking prolyl hydroxylase domain protein 2. *Mol Cell Biol.* 2006;26:8336–8346.
22. Nishimura S, Manabe I, Nagasaki M, Hosoya Y, Yamashita H, Fujita H, Ohsugi M, Tobe K, Kadowaki T, Nagai R, Sugiura S. Adipogenesis in obesity requires close interplay between differentiating adipocytes, stromal cells, and blood vessels. *Diabetes.* 2007;56:1517–1526.
23. Weisberg SP, McCann D, Desai M, Rosenbaum M, Leibel RL, Ferrante AW Jr. Obesity is associated with macrophage accumulation in adipose tissue. *J Clin Invest.* 2003;112:1796–1808.
24. Xu H, Barnes GT, Yang Q, Tan G, Yang D, Chou CJ, Sole J, Nichols A, Ross JS, Tartaglia LA, Chen H. Chronic inflammation in fat plays a crucial role in the development of obesity-related insulin resistance. *J Clin Invest.* 2003;112:1821–1830.
25. Lum JJ, Bui T, Gruber M, Gordan JD, DeBerardinis RJ, Covello KL, Simon MC, Thompson CB. The transcription factor HIF-1alpha plays a critical role in the growth factor-dependent regulation of both aerobic and anaerobic glycolysis. *Genes Dev.* 2007;21:1037–1049.
26. Westerterp KR, Kayser B, Wouters L, Le Trong JL, Richalet JP. Energy balance at high altitude of 6,542 m. *J Appl Physiol.* 1994;77:862–866.
27. Westerterp-Plantenga MS, Westerterp KR, Rubbens M, Verwegen CR, Richelet JP, Gardette B. Appetite at "high altitude" [Operation Everest III (Comex-'97)]: a simulated ascent of Mount Everest. *J Appl Physiol.* 1999;87:391–399.
28. Reynolds RD, Lickteig JA, Deuster PA, Howard MP, Conway JM, Pietersma A, deStoppelaar J, Deurenberg P. Energy metabolism increases and regional body fat decreases while regional muscle mass is spared in humans climbing Mt. Everest. *J Nutr.* 1999;129:1307–1314.
29. Gatenby RA, Gillies RJ. Why do cancers have high aerobic glycolysis? *Nat Rev Cancer.* 2004;4:891–899.
30. Zhong L, D'Urso A, Toiber D, Sebastian C, Henry RE, Vadysirisack DD, Guimaraes A, Marinelli B, Wikstrom JD, Nir T, Clish CB, Vaitheesvaran B, Iliopoulos O, Kurland I, Dor Y, Weissleder R, Shirihai OS, Ellisen LW, Espinosa JM, Mostoslavsky R. The histone deacetylase Sirt6 regulates glucose homeostasis via Hif1alpha. *Cell.* 2010;140:280–293.
31. Leguisamo NM, Lehnen AM, Machado UF, Okamoto MM, Markoski MM, Pinto GH, Schaan BD. GLUT4 content decreases along with insulin resistance and high levels of inflammatory markers in rats with metabolic syndrome. *Cardiovasc Diabetol.* 2012;11:100.
32. Ye J. Emerging role of adipose tissue hypoxia in obesity and insulin resistance. *Int J Obes (Lond).* 2009;33:54–66.
33. Yin J, Gao Z, He Q, Zhou D, Guo Z, Ye J. Role of hypoxia in obesity-induced disorders of glucose and lipid metabolism in adipose tissue. *Am J Physiol Endocrinol Metab.* 2009;296:E333–E342.
34. Hosogai N, Fukuhara A, Oshima K, Miyata Y, Tanaka S, Segawa K, Furukawa S, Tochino Y, Komuro R, Matsuda M, Shimomura I. Adipose tissue hypoxia in obesity and its impact on adipocytokine dysregulation. *Diabetes.* 2007;56:901–911.
35. Trayhurn P, Wang B, Wood IS. Hypoxia in adipose tissue: a basis for the dysregulation of tissue function in obesity? *Br J Nutr.* 2008;100:227–235.
36. Halberg N, Khan T, Trujillo ME, Wernstedt-Asterholm I, Attie AD, Sherwani S, Wang ZV, Landskroner-Eiger S, Dineen S, Magalang UJ, Brekken RA, Scherer PE. Hypoxia-inducible factor 1alpha induces fibrosis and insulin resistance in white adipose tissue. *Mol Cell Biol.* 2009;29:4467–4483.
37. Shimba S, Wada T, Hara S, Tezuka M. EPAS1 promotes adipose differentiation in 3T3-L1 cells. *J Biol Chem.* 2004;279:40946–40953.
38. Zhang X, Lam KS, Ye H, Chung SK, Zhou M, Wang Y, Xu A. Adipose tissue-specific inhibition of hypoxia-inducible factor 1{alpha} induces obesity and glucose intolerance by impeding energy expenditure in mice. *J Biol Chem.* 2010;285:32869–32877.
39. Zhang N, Fu Z, Linke S, Chicher J, Gorman JJ, Visk D, Haddad GG, Poellinger L, Peet DJ, Powell F, Johnson RS. The asparaginyl hydroxylase factor inhibiting HIF-1alpha is an essential regulator of metabolism. *Cell Metab.* 2010;11:364–378.
40. Furuhashi M, Hotamisligil GS. Fatty acid-binding proteins: role in metabolic diseases and potential as drug targets. *Nat Rev Drug Discov.* 2008;7:489–503.

CLINICAL PERSPECTIVE

Obesity is associated with low-grade chronic inflammation, dysregulated adipocytokine production, and increased oxidative stress in visceral adipose tissue, which is believed to result in insulin resistance, high blood pressure, and acceleration of atherosclerosis. Although hypoxia has long been known to reduce body weight in both humans and animals, the role of the hypoxia response system, including hypoxia-inducible factor and an oxygen sensor, prolyl hydroxylase domain protein (PHD), in the regulation of fat mass and glucose metabolism remains controversial. Therefore, in the present study, we sought to determine whether deletion of PHD2, a main isoform of PHD, in adipose tissue affects high-fat diet–induced obesity and glucose intolerance. We showed that PHD2 deficiency in adipocyte resulted in upregulation of hypoxia-inducible factor and attenuated high-fat diet–induced body weight gain and glucose intolerance compared with control mice. These effects seemed to be mediated by upregulation of glycolytic enzymes in white adipose tissue and uncoupling protein-1 in brown adipose tissue in the PHD2-deficient mice. The PHD2-deficient mice also showed modest improvement in insulin sensitivity. The improvement in glucose metabolism is associated with a decrease in adipocyte size, macrophage infiltration, and abnormal angiogenesis of white adipose tissue in the PHD2-deficient mice. Because of the worldwide pandemic of obesity and diabetes mellitus, a novel strategy that is effective for the treatment of both conditions has been sought. The present study suggests that PHD2 inhibition in adipocyte may be a new therapeutic approach to reduce body weight and to improve glucose tolerance simultaneously.

SUPPLEMENTAL MATERIAL

Supplemental File for Supplemental Methods, Supplemental Tables, Supplemental Figures (1-4) and Legends for Supplemental Figures.

Supplemental Methods

Materials

Dulbecco's Modified Eagle Medium (DMEM) was purchased from GIBCO BRL-Invitrogen Co. (Carlsbad, CA, U.S.A.). Fetal bovine serum (FBS) was purchased from SAFC Biosciences Inc. (Lenexa, KS, U.S.A.). A mouse monoclonal anti-α-tubulin antibody was purchased from Sigma-Aldrich Co. (St. Louis, MO, U.S.A.). Horseradish peroxidase-conjugated secondary antibodies (anti-rabbit and anti-mouse IgG) were purchased from Vector Laboratories, Inc. (Burlingame, CA, U.S.A.). Luciferase assay system was purchased from Promega Co. (Madison, WI, U.S.A.). Other chemical reagents were purchased from Wako Pure Chemical Industries, Ltd. (Osaka, Japan) unless otherwise stated.

Generation of adipocyte-specific PHD2-deficient mice.

To knockout *Phd2* gene in adipocytes, previously generated *Phd2*-floxed mice were used ($Phd2^{f/+}$).[1] Transgenic mice expressing Cre recombinase under control of *aP2* gene promoter (*aP2-Cre*) were purchased from the Jackson Laboratory (Stock Number 5069, Bar Harbor, Maine). $Phd2^{f/+}$ mice were crossed with *aP2-Cre* mice to obtain $Phd2^{f/+}$/*aP2-Cre* mice. Then, mice with PHD2 deletion in adipocyte ($Phd2^{f/f}$/*aP2-Cre*) were generated by stepwise crossing of $Phd2^{f/+}$/*aP2-Cre* mice with $Phd2^{f/f}$ mice. $Phd2^{f/f}$ mice were served as controls. The primers to detect *Phd2*-floxed gene and *Cre* gene were previously described.[2] These mice were fed a

high-fat diet (HFD) containing 60% kcal fat (High Fat Diet 32, Clea Japan) from 12 weeks to 18 weeks. Mice at the age of 12- and 18-week-old were analyzed. All procedures were approved by Animal Care and Use Committee, Kyushu University and conducted in accordance with the institutional guidelines.

Histological analysis

Adipose tissues were fixed in 10% neutral buffered formaldehyde solution overnight and embedded in paraffin. Paraffin sections were stained with hematoxylin and eosin (H&E). Ten images of H&E stained sections were acquired from each animal and cross-sectional area of each adipocyte was determined using the software Dynamic cell count BZ-HIC (Keyence, Japan). To detect macrophage infiltration, the paraffin sections were immunohistochemically stained with an anti-mouse Mac-3 antibody (Santa Cruz Biotechnology, Inc., Santa Cruz, CA) and detected with DAB chromogen. For morphological analysis of blood vessels, adipose tissues were minced with scissors to small pieces (1~2 mm) and the tissues were directly stained with FITC-Conjugate *Bandeiraea simplicifolia* lectin (Sigma Sigma-Aldrich Co., St. Louis, MO, U.S.A.) for two hours at room temperature. Then, the tissues were counterstained with 4',6-diamino-2-phenylindole (DAPI) and examined using the confocal laser scanning microscope A1R (Nikon, Japan). Capillary density was determined by counting blood vessels intersecting 1 mm line drawn in the photos of lectin-stained adipose tissues.

Glucose tolerance test and insulin tolerance test

Mice were starved for 6 hours.[3] For glucose tolerance test, mice were injected intraperitoneally with glucose (1 g/kg of body weight). For insulin tolerance test, mice were injected intraperitoneally with rapid insulin (0.5 IU/kg of body weight). Blood sample was taken from tail

vein at various time points and blood glucose concentrations were determined by using Glutest Every (Sanwa Kagaku Kenkyusho, Japan).

Measurement of serum levels of triglyceride, cholesterol, insulin, lactate and cytokines.

Serum triglyceride and total cholesterol levels were determined by commercially available kits, Triglyceride E-test Wako (Wako) and Cholesterol E-test Wako (Wako), respectively. Serum insulin levels were determined by insulin ELISA kit (Morinaga Institute of Biological Science, Japan). Serum lactate level was determined by lactate assay kit (BioVision, Mountain View, CA). Serum cytokine levels were determined by ELISA kits (R&D systems Inc. Minneapolis, MN, USA).

Western blot analysis

Protein preparation and Western blot analysis for PHD2,[1] HIF-1α, HIF-2α (Novus Biologicals, Littleton, CO USA), lactate dehydrogenase (LDH) a, Glut 4, Akt and phospho-Akt (Cell Signaling Technology, Danvers, MA, USA) were performed as described previously.[2] α-tubulin (Sigma-Aldrich Co.) or cyclic AMP response element binding protein (CREB, Cell Signaling Technology) was used as a loading control.

Isolation of adipocyte-enriched fraction and stromal vascular fraction (SVF) from white adipose tissues (WAT)

The epididymal fat tissue was minced and digested with collagenase (3 mg/ml, Sigma) in phosphate-buffered saline supplemented with bovine serum albumin (2%, Sigma) at 37 °C for 60 minutes with gentle agitation. Then, the digested fat tissues were filtered through a 250 μm nylon mesh and centrifuged at 430 g for 1 minutes. The sediments were used as a SVF and floating

cells were used as an adipocyte-enriched fraction after washing with PBS for several times.

Isolation of bone marrow derived macrophages (BMDM).

Bone marrow cells were isolated from femurs and tibias, and were centrifuged (1000rpm, 5 min, 4°C). The sediments were resuspended in DMEM supplemented with 10% FBS and 30% L929 conditioned medium as a source of M-CSF for 7days and attached cells were used as BMDM.[4]

Oxygen consumption measurement.

Mice were fed a HFD, maintained at a constant room temperature (21–23°C), and subjected to oxygen consumption measurements using a computer-controlled open-circuit indirect calorimeter (Oxymax; Columbus Instruments, Columbus OH) during the light period (8 a.m. to 8 p.m.) and the dark period (8 p.m. to 8 a.m.). Mice were housed individually in metabolic chamber. After a 1 hour adaptation to the chamber, VO_2 was assed at 4-min intervals for 24 hours. All sample data were analyzed using Oxymax Windows software (version 1.0).

Cell culture

3T3-L1 murine preadipocytes were purchased from Human Science Research Resources Bank (Japan). The cells were maintained in low-glucose DMEM culture medium supplemented with 10 % FBS in an atmosphere of 5 % CO_2 at 37 °C. To differentiate 3T3-L1 preadipocytes into adipocytes, the cells were cultured with high-glucose DMEM containing 10 % FBS, 10 μg/ml insulin, 0.25 μmol/L dexamethasone, and 500 μmol/L isobutylmethylxanthine for two days. Then, the cells were cultured with fresh high-glucose DMEM containing 10 % FBS and 10 μg/ml insulin for additional two days. After that, the cells were maintained in DMEM containing 10% FBS for another 8 days.

Gene silencing by retrovirus-mediated small hairpin (sh) RNA expression

Expression vectors of shRNA specific for *Phd2* gene were generated using pSINsi-hU6 vector containing the neomycin resistant gene under control of SV40 promoter (Takara Biotechnology, Shiga, Japan). Target DNA sequences for shRNA specific for *Phd2* gene were 5'-GCAATAACTGTTTGGTATT-3'. The DNA sequence of control shRNA which had no similarity for any murine genes was 5'- TCAGAACGATGACTGAGAG-3'. The constructs were introduced to Plat-E cells (Cell Biolabs, San Diego, CA, USA) with FuGene6 transfection reagent (Roche Applied Science, Basel, Switzerland). After 48 hours, the culture medium containing retrovirus particles was collected and filtered by passing through 0.45 μm filter (Schleicher&Schuell, Dassel, Germany). Then 3T3-L1 cells were infected with the retrovirus for 24 hours and subsequently selected by G418 (500 μg/ml) treatment for another 7 days.

Oil Red O staining

To determine the extent of lipid accumulation in cytosol, differentiated 3T3-L1 adipocytes were fixed with 10 % formaldehyde for 10 minutes and stained with 0.18 % Oil Red O solution for 15 minutes. After staining, the cells were rinsed with 60% isopropanol. After taking photos, the dye was extracted with 100% isopropanol and absorbance at 520 nm was measured.

RNA extraction and real-time quantitative RT-PCR (qPCR) analysis

RNA from adipose tissue, quadriceps femoris muscle, liver, and cultured cells was extracted using ISOGEN according to manufacturer's instruction (Wako Pure Chemical Industries, Ltd.). One μg of total RNA was reverse-transcribed using ReverTra Ace qPCR RT Kit (TOYOBO, Osaka, Japan). Real-time qPCR was performed using 7500 real-time PCR system (Life Technologies Co., Carlsbad, CA, U.S.A.) and SYBR Green PCR Master Mix (Life Technologies Co.). The expression of each gene was normalized with either *hypoxanthine phosphoribosyltransferase* (*Hprt*), *β-actin* expression or 18S rRNA. Primer sequences are summarized in the Supplemental Table 1.

Measurements of transcriptional activity of HRE-driven promoter

A luciferase construct with 7 copies of hypoxia responsive element (HRE) was a generous gift from Dr. Masaomi Nangaku (University of Tokyo, Japan). The HRE-luciferase vector was introduced to 3T3-L1 preadipocytes by the DEAE-dextran method according to the manufacturer's instructions (Promega Corporation, Madison, WI, U.S.A.). The luciferase activity was measured by Lumat LB9501 (Berthold, Bad Wildbad, Germany) and normalized with protein concentrations.

Statistical analysis

Normality and homoskedasticity of the data were assessed by Shapiro-Wilk test and Levene test, respectively. A *t*-test was used for comparing two groups. Differences between multiple groups were evaluated using one-way ANOVA followed by Fisher's post hoc test if appropriate. The data on the number of crown-like structure (Figure 3C) and vascular density (Figure 3I) were assessed by exact binomial test. The data on insulin tolerance test and glucose tolerance test were analyzed by repeated measure two-way ANOVA. Data are shown as mean±SEM. $P<0.05$ was considered to be statistically significant.

References for the methods.

1. Takeda K, Ho VC, Takeda H, Duan LJ, Nagy A, Fong GH. Placental but not heart defects are associated with elevated hypoxia-inducible factor alpha levels in mice lacking prolyl hydroxylase domain protein 2. *Mol Cell Biol*. 2006;26:8336-8346
2. Takeda K, Cowan A, Fong GH. Essential role for prolyl hydroxylase domain protein 2 in oxygen homeostasis of the adult vascular system. *Circulation*. 2007;116:774-781
3. Andrikopoulos S, Blair AR, Deluca N, Fam BC, Proietto J. Evaluating the glucose tolerance test in mice.*Am J Physiol.* 2008;295:E1323-1332

4. Weischenfeldt J, Porse B. Bone marrow-derived macrophages (bmm): Isolation and applications. *CSH protocols*. 2008;2008:pdb prot5080

Supplemental table 1. Sequences of the primers used for real-time qPCR

mRNA	Forward primer	Reverse primer
Aco	5'- AAGATGGATCCTAAGCCAGCTGAA-3'	5'- CAGCTTACCACAAAGCCAGCTACTC-3'
Adiponectin	5'-GTCAGTGGATCTGACGACACCAA-3'	5'-ATGCCTGCCATCCAACCTG-3'
β-actin	5'-GGCTGTATTCCCCTCCATCG-3'	5'-CCAGTTGGTAACAATGCCATGT-3
C/EBPα	5'-TTGAAGCACAATCGATCCATCC-3'	5'-GCACACTGCCATTGCACAAG-3
Cpt1a	5'- GAAGCCTTTGGGTGGATATGTGA-3'	5'- ATGGAACTGGTGGCCAATGA-3
Dec1	5'-GGAGGTGACTCACAGCAGACTGAC-3'	5'- GCAGAAATTTGCCCAAACCA-3'
Fgf2	5'- GTGCCAACCGGTACCTTGCTA-3'	5'- TCAGTGCCACATACCAACTGGAG-3'
Gapdh	5'-TGTGTCCGTCGTGGATCTGA-3'	5'-TTGCTGTTGAAGTCGCAGGAG-3'
Glut1	5'- CTTCATTGTGGGCATGTGCTTC-3'	5'-AGGTTCGGCCTTTGGTCTCAG-3
Glut4	5'-CTGTAACTTCATTGTCGGCATGG-3'	5'-AGGCAGCTGAGATCTGGTCAAAC-3'
G6pase	5'- GGATCCTGGGACAGACACACAA-3'	5'- ATGTCAACACCTCTGGCCTCAC-3'
Hprt	5'- TTGTTGTTGGATATGCCCTTGACTA -3'	5'-AGGCAGATGGCCACAGGACTA-3'
Il-6	5'-CCACTTCACAAGTCGGAGGCTTA-3'	5'-GCAAGTGCATCATCGTTGTTCATAC-3'
Ldha,	5'- GGATGAGCTTGCCCTTGTTGA-3'	5'-GACCAGCTTGGAGTTCGCAGTTA-3'
MCAD	5'- TGATGTGGCGGCCATTAAGA-3'	5'- CGGCTTCCACAATGAATCCAG-3'
Mcp1	5'-TTAACGCCCCACTCACCTGCTG-3'	5'-GCTTCTTTGGGACACCTGCTGC-3'
Pepck1	5'- TCTTTGGTGGCCGTAGACCTG-3'	5'- GCCAGGTATTTGCCGAAGTTGTAG-3'
Pdk1	5'-GCTACGGGACAGATGCGGTTA-3'	5'-CAGGCGGCTTTATTGTACACAGG-3'
Plgf,	5'- CCTGTCTGCTGGGAACAACTCA-3'	5'- CACCTCATCAGGGTATTCATCCAAG-3'
Pgk1	5'-TGGATGAGGTGGTGAAAGCC-3'	5'-GCACAGCAAGTGGCAGTGTC-3'
Phd1	5'-CATCAATGGGCGCACCA-3'	5'-GATTGTCAACATGCCTCACGTAC-3'
Phd2	5'-TAAACGGCCGAACGAAAGC-3'	5'-GGGTTATCAACGTGACGGACA-3'
Phd3	5'-CTATGTCAAGGAGCGGTCCAA-3'	5'GTCCACATGGCGAACATAACC-3'
Pparγ	5'-TGTCGGTTTCAGAAGTGCCTTG-3'	5'-TTCAGCTGGTCGATATCACTGGAG-3'
Tnf-a	5'-CATCTTCTCAAAATTCGAGTGACAA-3'	5'-TGGGAGTAGACAAGGTACAACCC-3'
Ucp1	5'- TACCAAGCTGTGCGATGTCCA3'	5'- GCACACAAACATGATGACGTTCC-3'
Vegf-a	5'-GCACATAGGAGAGATGAGCTTCC-3'	5'-CTCCGCTCTGAACAAGGCT-3'
18S rRNA	5'-ACTCAACACGGGAAACCTCA-3'	5'-AACCAGACAAATCGCTCCAC-3'

Abbreviations

Aco; acyl CoA oxidase

C/EBP; CCAAT/enhancer binding protein

Cpt1a; carnitine palmitoyltransferase-1

DEC1; differentiated embryo chondrocyte 1

Fgf ; fibroblast growth factor

Gapdh ; glyceraldehyde-3-phosphate dehydrogenase

Glut ; glucose transporter

G6pase; glucose-6-phosphatase

Hprt ; hypoxanthine phosphoribosyltransferase

Il ; interleukin

Ldh ; lactate dehydrogenase

MCAD; medium chain acyl-CoA dehydrogenase

Mcp ; monocyte chemoattractant protein

Pepck; phosphoenolpyruvate carboxykinase

Pdk ; pyruvate dehydrogenase kinase

Plgf ; placental growth factor

Pgk ; phosphoglycerate kinase

Phd ; prolyl hydroxylase domain protein

Ppar ; peroxisome proliferator activated receptor

Tnf ; tumor necrosis factor

Ucp; uncoupling protein

Vegf ; vascular endothelial growth factor

Supplemental Table 2. Organ weight of control and *Phd2*$^{f/f}$ / *aP2-Cre* mice.

Organs	Control (n=6)	*Phd2*$^{f/f}$ / *aP2-Cre* (n=6)	*p* values
Epididymal fat (mg)	1208 ± 50	758 ± 35	*P*<0.01
Perirenal fat (mg)	647± 35	366 ± 26	*P*<0.01
Liver (mg)	1496 ± 117	1229 ± 105	*P*=0.12
Heart (mg)	178 ± 3	190 ± 12	*P*=0.35
Spleen (mg)	108 ±10	100 ± 20	*P*=0.35
Kidney (mg)	200 ±10	176 ± 5	*P*=0.06

Supplemental Figure 1

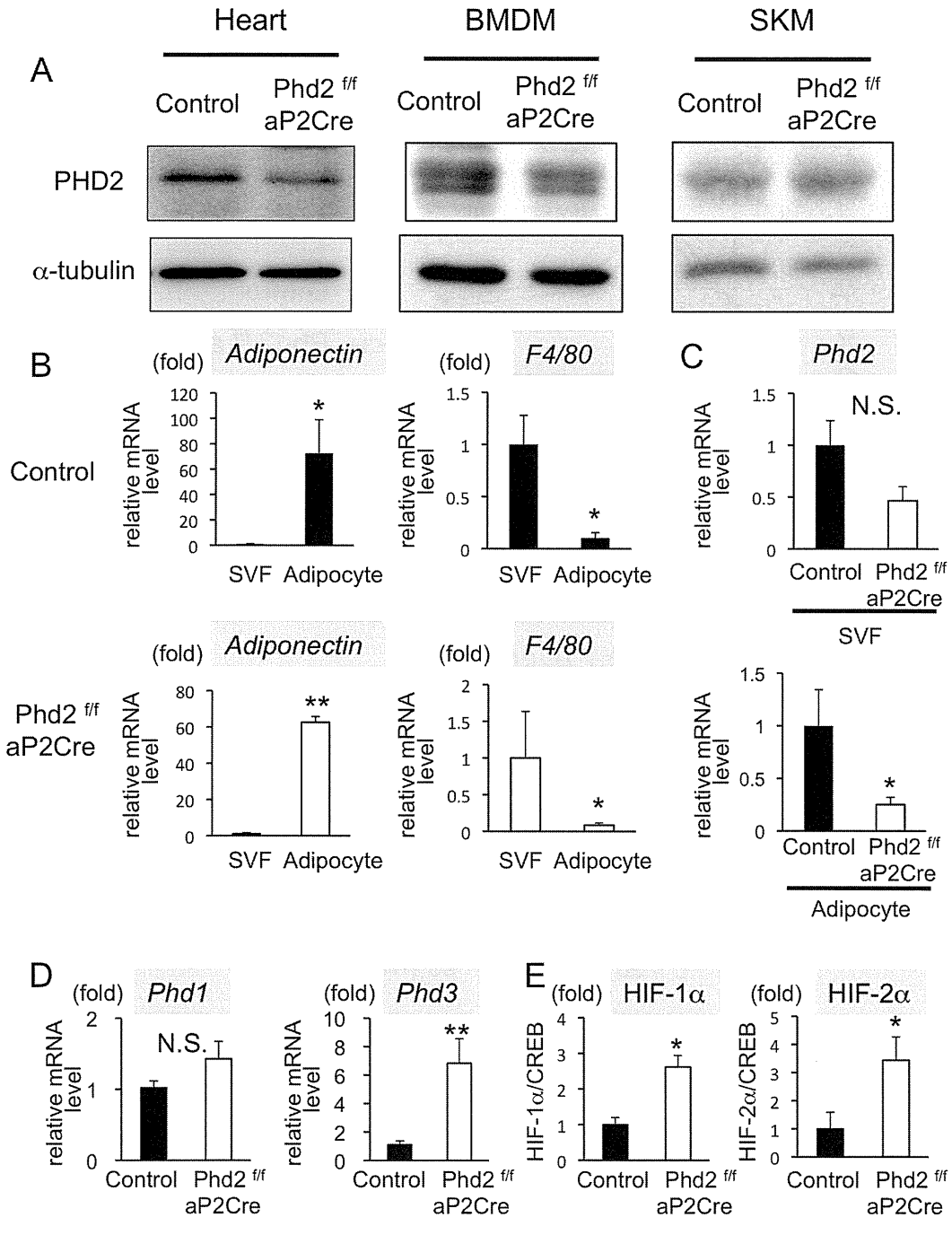

Supplemental Figure 2

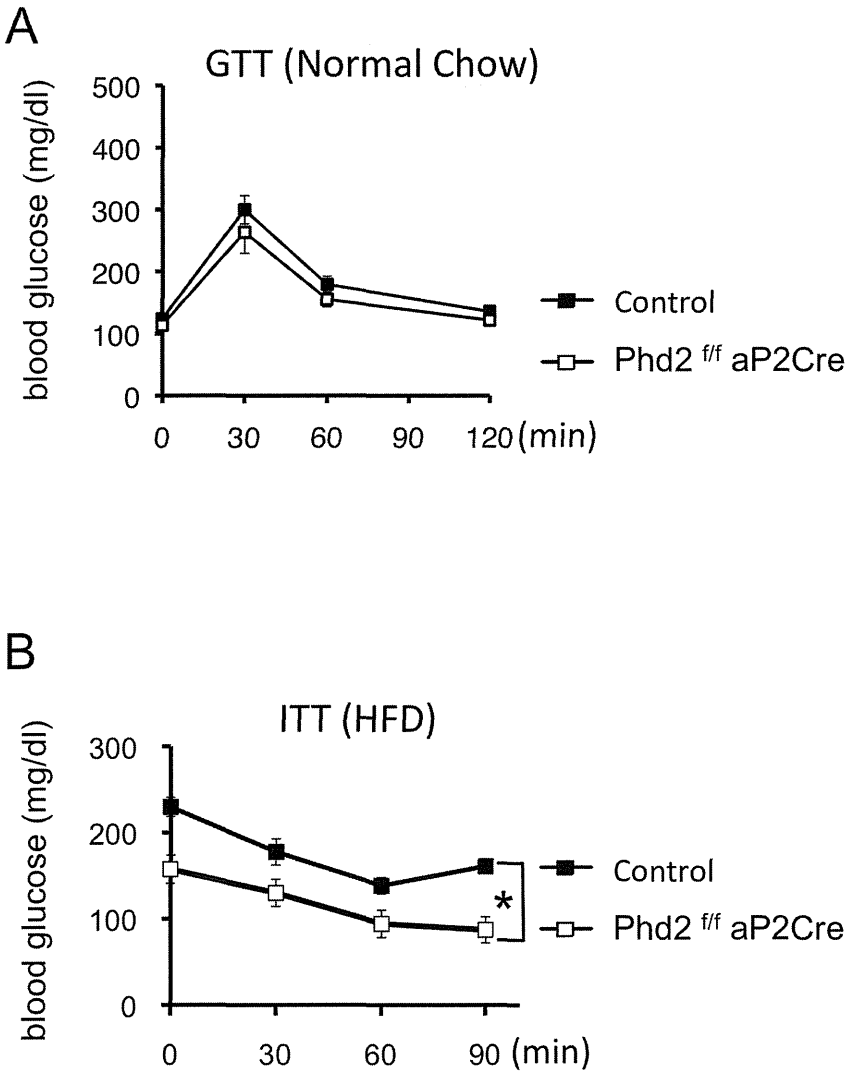

Supplemental Figure 3

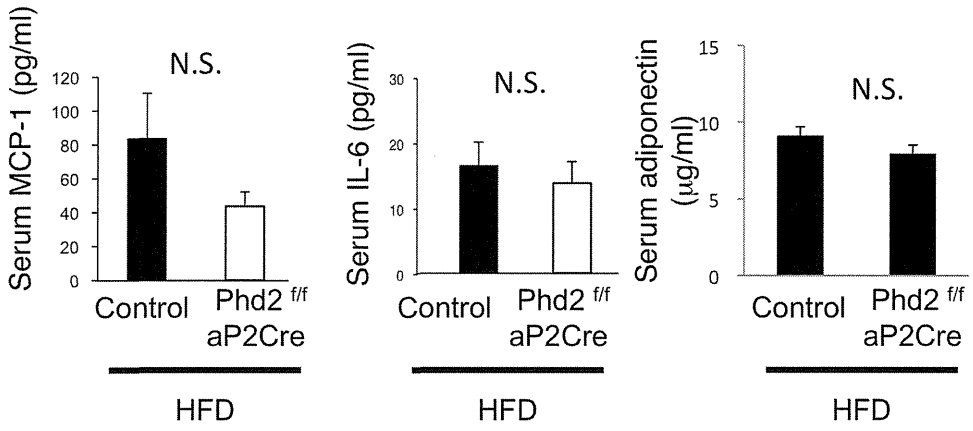

Supplemental Figure 4